Indonesian Journal of Electrical Engineering and Computer Science
Vol. 30, No. 2, May 2023, pp. 707~713
ISSN: 2502-4752, DOI: 10.11591/ijeecs.v30.i2.pp707-713

Effects of (Ba,Ca)ScO_2F:Bi^3+,K^+ phosphor particle size on color uniformity white light-emitting diodes

Ha Thanh Tung[1], Huu Phuc Dang[2]
[1]Faculty of Basic Sciences, Vinh Long University of Technology Education, Vinh Long Province, Vietnam
[2]Faculty of Fundamental Science, Industrial University of Ho Chi Minh City, Ho Chi Minh City, Vietnam

Article Info

Article history:

Received Sep 7, 2022
Revised Nov 10, 2022
Accepted Nov 19, 2022

Keywords:

(Ba,Ca)ScO_2F:Bi^{3+},K^+
LED devices
Luminescent
Phosphors
Spectrum

ABSTRACT

Phosphors that offer considerable performance as well as heat consistency has been a high priority of recent studies concerning light-emitting diodes (LED) devices. This study employs the perovskite phosphors BCSOF (short for $Ba_{1-x}Ca_xScO_2F$:0.001Bi3+,0.001K+ with x value from 0 to 0.12 and one chip at 415 nm generating thin green illumination via cation-replacement method. The study examines the aftermath when Ca^{2+} replaces Ba^{2+} within the crystal formations of BCSOF as well as the luminescent features of the phosphors, detecting a formation of cube-like perovskite within the space group of Pm3m in the employed phosphors. In addition, the study also assesses the development concerning the magnitude of cells as well as the binding extent of Ba/Ca/K/Bi-O. When the inner quantum performance reaches 77.4% in BCSOF, a potent green discharge is manifested, reaching 510 nm when excited by a chip at 415 nm. Greater luminescent performance as well as heat consistency correlating with changes in inner formation were reported. Via the method of replacing cations, it is possible to control spectrum by manipulating the latticework's surroundings, leading to desirable performance in LED products.

Corresponding Author:

Huu Phuc Dang
Faculty of Fundamental Science, Industrial University of Ho Chi Minh City
No. 12 Nguyen Van Bao Street, Ho Chi Minh City, Vietnam
Email: danghuuphuc@iuh.edu.vn

1. INTRODUCTION

The phosphor-converted white-light-emitting diode (pc-WLEDs), short for phosphor-converted white light emitting diodes, are commonly seen as suitable apparatuses when it comes to optical exhibition [1], [2]. Compared to older lighting devices, the pc-WLEDs carry various benefits such as extended time of use, high reliability, and low power consumption. Creating WLED devices usually requires a merger between yellow phosphor YAG:Ce^{3+}, one blue InGaN light-emitting diodes (LED) chip and red phosphor $(Sr,Ca)_2Si_5N_8$:Eu^{2+} [3], [4]. On the other hand, this method is not particularly practical, due to full width at half maximum (FWHM) values for YAG:Ce^{3+} and $(Sr,Ca)_2Si_5N_8$:Eu^{2+} exceeding 100 nm and 90 nm, respectively. In addition, the insufficient green discharge causes a hue scale of merely around 80% based on the national television system committee criteria (NTSC) and also harms the hue authenticity [5], [6]. Hence, acquiring thin-line green phosphor that offers significant heat consistency would be vital. The criteria of WLED devices requires said phosphors to have superior hue scale [7], [8]. The method of replacing cations would be useful for task of creating phosphors that offer desirable photoluminescent features, which may include red or blue shift alteration for the location of discharge apex, superior luminescent performance and heat consistency [9]–[11]. Generally, it is possible to create phosphors having superior features of luminescent via replacing cations.

For this study, green phosphors yielding excitation wavelength reaching 415 nm were examined. The study utilizes the method of replacing cation to create BCSOF via $BaScO_2F:Bi^{3+},K^+$. We replaced the ions of Ba^{2+} with the ions of Ca^{2+} to acquire multiple BCSOFs and examined formation development, form, absorption spectra, luminescent features with or without reliance on temperature, as well as the performance of LED device. We also examined the result of augmenting luminescent intensity, discharge line's redshift as well as heat consistency via managing micro-formation. Ultimately, we managed to create one WLED device yielding 110% NTSC hue scale by incorporating BCSOF. As such, this phosphor may prove effective when utilized in WLED devices.

2. METHOD

2.1. Creating BCSOF ($Ba_{1-x}Ca_xScO_2F:0.001Bi^{3+},0.001K^+$)

Using the solid-state technique under high temperature, we created the BCSOF samples with x values of 0, 0.03, 0.06, 0.09, 0.12. The materials required for the creation process will be detailed in Table 1. Certain steps of the process will also be shown by the Table 1 [12]–[14].

Table 1. Constituents and creation process of BCSOF

Materials	Purity	Process
BaCO3	99.99%	– Combine predetermined amounts of all materials
BaF2	99.99%	– Calcinate the acquired substance under the temperature of 1,200 ^{0}C within eight hours inside a furnace [14]
Sc2O3	99.99%	
CaCO3	99.99%	– Calcinate the substance under the temperature of 1,100 ^{0}C within four hours under a lowering atmosphere with gas containing 10% H2 and 90% N2, resulting in ions of Bi in three-valence condition
Bi2O3	99.99%	
K2CO3	99.99%	– Let the substance cool down, then pulverize it

2.2. Characteristics of the phosphor samples

Following the creation process of BCSOF samples, we proceeded to examine their characteristics. For this task, various tools were employed. The characteristics and their matching tools is detailed in Table 2 [15].

Table 2. Characteristics and determining tools

Characteristics	Tools
Crystal formation	X-ray diffractometry with Cu-Kα radiation under 30 kilovolts and 20 milliamperes
Formation rectification	GSAS program
Micro-formation and elemental configuration	Scanning electron microscopy and energy dispersive spectrometry
Absorption spectra between 200 nm and 800 nm	UV-VIS-NIR spectrophotometer
Photoluminescent and photoluminescent excitation spectra	Fluorescent spectrophotometer accompanied by Xe light under 150 watts and room temperature
Inner quantum performance	F-7000 having one Quanta-φ globe as well as one polytetrafluoroethylene sample cup
Luminescent features reliant on temperature	FLS980 spectrometer accompanied by Xe light under 450 watts in the form of excitation cause
Lifetimes	FLS920 spectrometer accompanied by nanosecond flash lamp in the form of excitation cause
Photoelectric features in WLED device (photoluminescent spectra, hue coordinates, CRI - color rendering index)	Integrating globe method [13]

3. RESULTS AND DISCUSSION

Figure 1 will detail the phosphor attributes through assessments. Figure 1(a) demonstrates the XRD (short for X-ray diffraction) activities in every samples of BCSOF [16]. As can be seen in Figure 1(b) and Figure 1(c), every diffractions apexes match apexes in $BaScO_2F$, which indicates pure stage development. As such, the primary stage formation remains the same when Bi^{3+}, K^+, and Ca^{2+} are co-doped, which results in BCSOF. As Ca^{2+} content surges in Figure 1(b), every diffraction apexes move towards greater angles, resulting from Ca^{2+} ion with lesser radius taking the place of Ba^{3+} (1.34 Å compared to 1.61 Å). The Bragg expression will demonstrate the alterations of XRD activities [17]:

$$2d \sin\theta = n\lambda \quad (1)$$

d indicates interplanar gap. λ indicates X-ray wavelength. θ indicates angle of diffraction. When the ions of Ca^{2+} take the place of the ions of Ba^{2+}, the unit cell along with the gap will become smaller. For the task of examining the disarray of formation, we utilized Rietveld rectification for XRD activities, demonstrated via Figures 1(d) and (e). Table 3 displays the crystal parameters for rectified BCSOF phosphors. The rectification appears to be consistent and accurate, as evidenced by the rectification's surplus factors (*R*) meeting at a low point. The parameter, along with the volume of cells, declines as the Ca^{2+} doping content surges. In Figure 1(f) and Figure 1(g), the binding scopes for d(Ba/Ca/Bi/K-O/F) assumed the value of 2.9440(5) Å, down from 2.9490(4) Å, as x surges. The ions of Ca^{2+} appear to alter polyhedron of $(Ba/Ca/Bi/K)O_{12}$, displaying smaller unit cell as Ca^{2+} content surges, which leads to lesser binding scopes of d(Ba/Ca/Bi/K-O/F). As such, altering the binding scope will alter the polyhedral of $[BiO_{12}]$ as well as the crystal field sturdiness for Bi^{3+}. The minor polyhedral movement may follow the forms of asymmetrical contact, and deformation, and leads to various deformations of polyhedral. Said deformation results from the asymmetrical contact for the bindings of (Bi-O). The expression will determine the polyhedral distortion index (*D*) [18]:

$$D = \frac{1}{n}\sum_{i=1}^{n}\frac{|d_i - d_{av}|}{d_{av}} \tag{2}$$

d_i indicates the range between the center atom and the *i*-th coordinating atom. d_{av} indicates the median scope for every binding. *D* reaches the values of 0.0009, up from 0.0049, as Ca^{2+} content surges in Figure 1(g). The greater deformation of polyhedral BiO_{12} will escalate crystal field cleavage for Bi^{3+}, causing a lesser shift for power level between $^1S_0$ and $^3P_1$.

The X-ray Rietveld rectification and the crystal formation for BCSOF can be seen in Figures 1(e) and (d), respectively, pointing out that the unit cell contains corner-linked $[Sc(O/F)_6]$ and the cation of Ba/Ca/Bi/K located at gap of octahedral accompanied by cuboctahedra of $[Ba/Ca/Bi/K(O/F)_{12}]$. The anion lesser latticework contains oxygen in disarray along with fluorine, forming a proportion of 67%: 33%. For the task of assessing the nature of Ca^{2+} substitution, the allowed variance of percentage for the radius of ions that are doped and replaced will remain at 25% or lower, with fault chemistry considered. The expression will determine the nature of substitution [19]:

$$D_{\mathrm{r}} = 100 \times \frac{[R_{\mathrm{m}}(\mathrm{CN}) - R_{\mathrm{d}}(\mathrm{CN})]}{R_{\mathrm{m}}(\mathrm{CN})} \tag{3}$$

D_r indicates the variance in percentage of radius. R_m and R_d indicate the radius for host cation as well as doped ion. Coordination number (CN) indicates value of coordination. The radius for doped ion of Ca^{2+} appears identical to that of Ba^{2+} (1.34 Å compared to 1.61 Å) with both having value of coordination equal to 12. The disparity of radius among said ions would be 16.6%, the limit. Therefore, with the distortion extent for $(Ba/Ca/Bi/K)O_{12}$ polyhedron altered by surging x value in Figure 1(e), it is possible to combine the ions of Ca^{2+} with $BaScO_2F$ so these ions can be substituted for Ba^{2+}.

Figure 2 exhibits the short for transmission electron microscopy (TEM) activities for $BaScO_2F$:0.001Bi^{3+},0.001K^+ and BCSOF, which is shown by the section Figures 2(a) and (b), respectively. Figures 2(c) and (d) displays the short for high-resolution transmission electron microscopy (HR-TEM) for $BaScO_2F$:0.001Bi^{3+},0.001K^+ and BCSOF, respectively [20]–[22]. The latter sample possesses a considerable crystallinity identical to $BaScO_2F$:Bi^{3+},K^+. The EDS spectrum and elemental activities for the samples are demonstrated by Figures 2(e) and (f), respectively, pointing out that Ba, Ca, Sc, O, F, Bi as well as K would be equally allocated among the granules of $BaScO_2F$. This suggests that the crystal latticework manages to receive Ca^{2+}, Bi^{3+} as well as K^+.

Figure 3 shows the relationship between the BCSOF and YAG:Ce^{3+} content. The findings imply that the correlation's primary goals are to maintain the median short for correlated color temperature (CCT) values and to have an impact on the WLED device's pair of phosphor sheets' absorptivity and dispersion [23], [24]. In light of the fact that the device's hue output depends on BCSOF concentration, there may be an effect on both lumen and hue output. The concentration of YAG:Ce^{3+} will decrease if the aforementioned concentration is increased (by 2% to 20%), allowing the median values of CCT to be maintained. Similar results will also be seen with WLED devices operating within the 5,600–8,500 K temperature range.

Figure 4 illustrates how the concentration of BCSOF might change the WLED device's transmitting spectrum. The demands of manufacturing must be taken into consideration while choosing a concentration. There are WLED products that provide a sizable colour output, resulting in a hardly decreased lumen. White illumination will result from a merging that produces a spectral zone. By comparing two optical spectrum regions between 420 and 480 nanometers as well as between 500 and 640 nanometers, it appears that an increase in BCSOF content will result in higher intensities. Superior luminous flux is indicated by the existence of a larger discharge spectrum. The phosphor sheet and the WLED device may both experience more active

dispersion as a result of the blue illumination's dispersion for the WLED device being more powerful. Such a result will subsequently improve the color constancy, a need for using BCSOF. When the objective is to control stated uniformity for a phosphor pattern under really high temperatures, it won't be easy. Our team's evaluation has shown that the BCSOF is beneficial for boosting the color output for WLED devices at temperatures of 8,500 K as well as 5,600 K. Our evaluation measured the lumen performance for the two-sheet remote phosphor arrangement.

The lumen experiences a significant jump as the BCSOF content increases to 20% wt. from 2%, as seen in Figure 5. According to Figure 6, the hue aberration experienced a pronounced penalty when the BCSOF concentration decreased under median CCT values. This outcome may be due to the layer of phosphor's absorptivity. As the blue lighting from the LED chip is absorbed by the blue phosphor granules, it is transformed into green light. In addition to the previously stated blue light, the BCSOF granules will also absorb yellow light. The phosphor's properties result in greater efficiency for the chip's ability to absorb blue light. Therefore, the green presence in the WLED device will be higher if we add BCSOF. The uniformity of the hue would be one of the most important aspects of WLED devices. The cost of the gadgets will be impacted by this uniformity. Due of BCSOF's cheap price, practical applications on a broad scale may result.

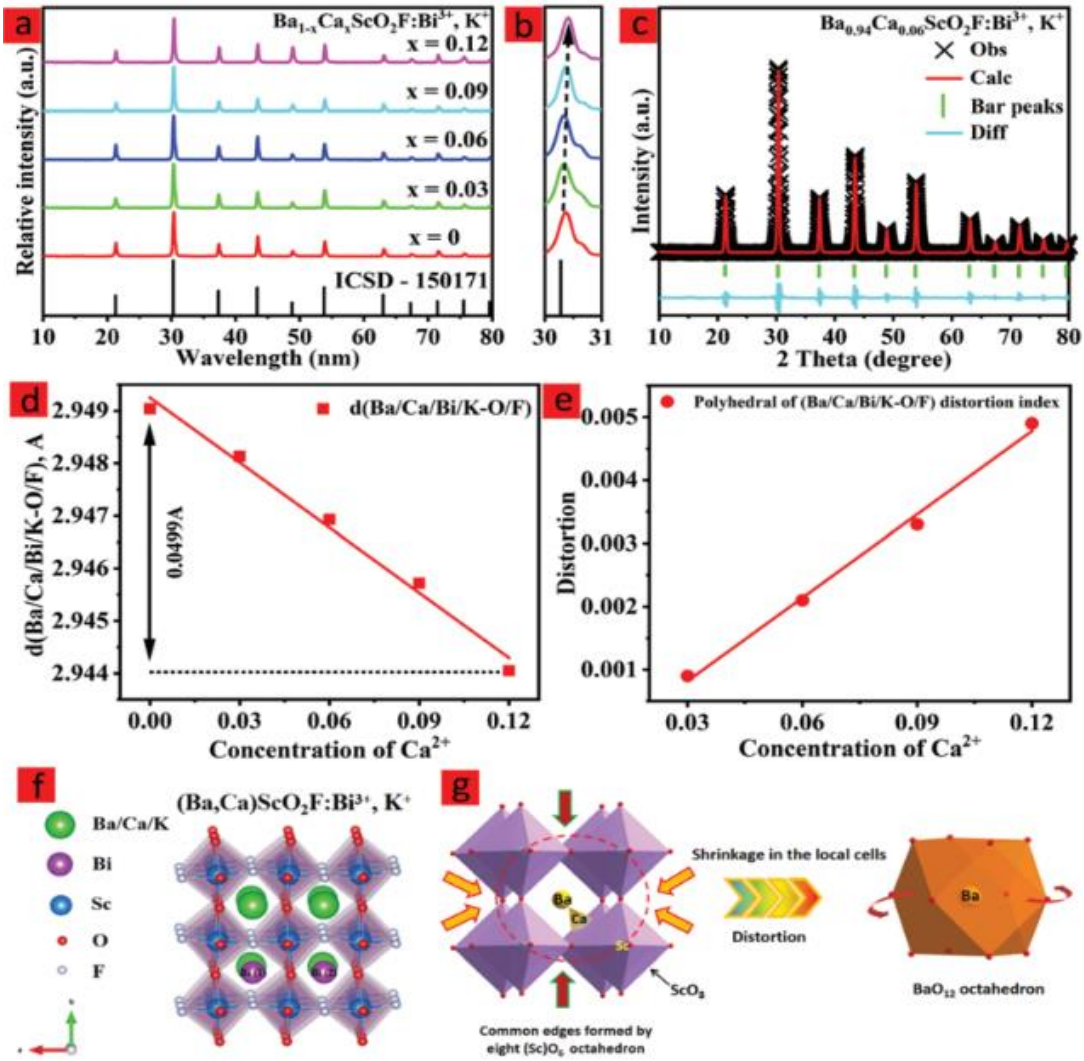

Figure 1. Assessment of phosphor attributes (a) XRD activities having, (b) noticeable presence between 30^0 and 31^0, (c) X-ray Rietveld rectification, (d) Binding scope d(Ba/Ca/Bi/K-O/F) altered as, (e) x surges, (f) Crystal formation in BCSOF, and (g) Effect on the surroundings of BaO12 from BCSOF as ion of Ca^{2+} is doped

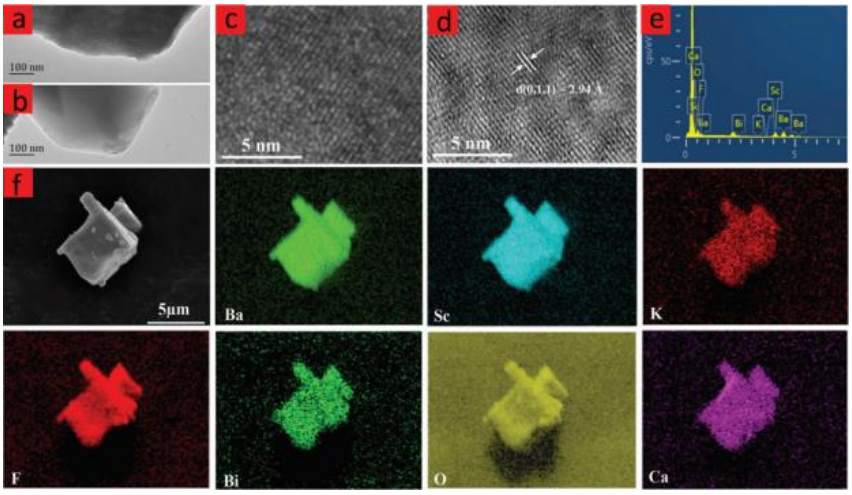

Figure 2. Additional phosphor attribute assessment (a) and (b) TEM display for $BaScO_2F$:0.001Bi^{3+},0.001K^+ and BCSOF respectively, (c) and (d) HRTEM display for $BaScO_2F$:0.001Bi^{3+},0.001K^+ and BCSOF respectively, (e) and (f) Phosphor's EDS spectrum along with elemental display

Table 3. Rectification outcomes and formational information for BCSOF

Rectified expression	x=0	x=0.03	x=0.06	x=0.09	x=0.12
Crystal formation	Cube	Cube	Cube	Cube	Cube
Space group	*Pm3m*	*Pm3m*	*Pm3m*	*Pm3m*	*Pm3m*
Cell parameter (Å)	4.1678(8)	4.1675(4)	4.1671(6)	4.1664(1)	4.1655(7)
Volume (Å3)	72.441(6)	72.421(4)	72.401(3)	72.386(5)	72.364(7)
Binding scope (Ba/Ca/Bi/K-O/F)	2.9490(4)	2.9481(3)	2.9469(3)	2.9457(2)	2.9440(5)
U_{iso} (Ba) (Å2)	0.0130(7)	-	0.0104(2)	-	-
R_p	6.37%	6.48%	6.54%	6.62%	6.73%
R_{wp}	9.22%	9.31%	9.47%	9.52%	9.61%

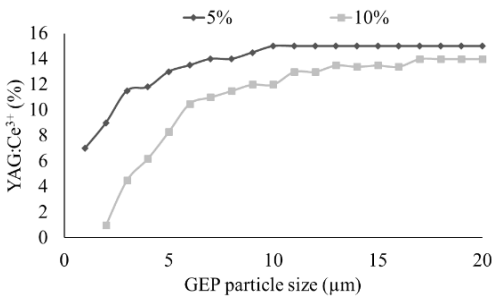

Figure 3. Modifying phosphor content and retaining median CCT

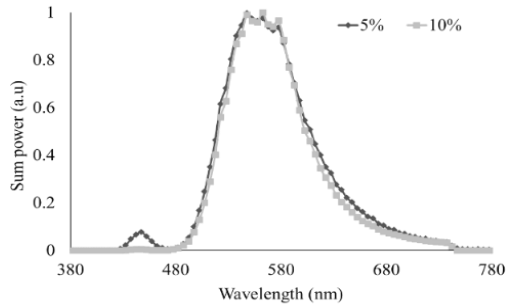

Figure 4. WLED's emission spectra along with BCSOF concentration

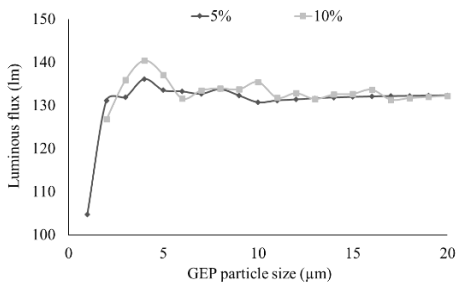

Figure 5. WLED's lumen along with BCSOF concentration

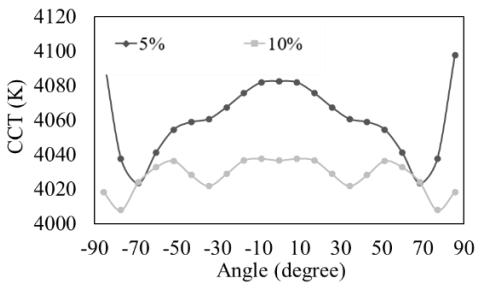

Figure 6. WLED's CCT along with BCSOF concentration

A common factor used to evaluate the color quality in WLED devices is hue consistency. However, this aspect only has a limited impact on the colour quality. An additional element that can evaluate both hue output and hue generation was developed in earlier studies. When an object is lighted, color rendering index (CRI) can identify its true color. The excessive amount of green illumination in comparison to the primary colours, which are blue, yellow, and green, is what causes the lack of chromatic uniformity. Such an occurrence may change the WLED device's color output, which would worsen hue consistency. Figure 7 shows how the value of CRI suffers a negligible cost when a BCSOF sheet is included. It is important to note how commonplace this punishment is. It is essential to concentrate on obtaining appropriate CQS values. This crucial aspect would be evaluated by CRI, observer bias, and hue coordinates, making it extremely helpful for assessing hue output [25]. Figure 8 shows how the presence of a BCSOF sheet causes a jump in color quality scale (CQS). If the BCSOF content increases while staying 10% wt., the factor would essentially remain unchanged. The waste of color brought on by green hue's dominance will cause CRI and CQS to significantly deteriorate in the case of 10% wt. or greater. This makes determining the optimal phosphor concentration before using BCSOF necessary.

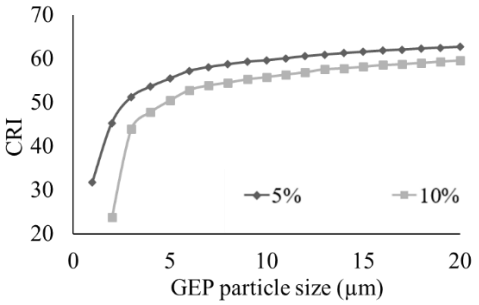

Figure 7. WLED's color rendering index (CRI) along with BCSOF concentration

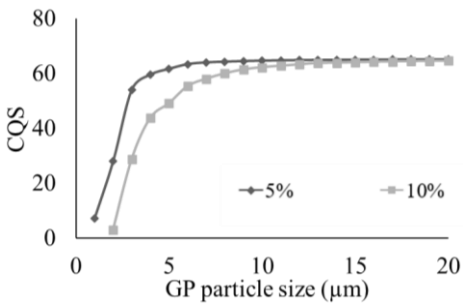

Figure 8. WLED's color quality scale (CQS) along with BCSOF concentration

4. CONCLUSION

This study focuses on the samples of BCSOF yielding 60-nm FWHM, which we created to applied in WLED devices by employing the method of replacing cation. A formation of cube-like perovskite within the space group of Pm3m was found in the samples. As the ions of Ba^{2+} are replaced by Ca^{2+} with lesser size, the formation becomes smaller, causing greater cleavage of crystal field. From here, it is possible to augment the luminescent intensity as well as heat consistency in BCSOF. Replacing cation may prove useful for manipulating photoluminescent spectrum through regulating the ion surrounding within the latticework of crystal. Ultimately, the study succeeded in creating one WLED apparatus that yields a significant 110% hue scale under 4,396 K. BCSOF has the potential to become an effective component for WLED devices.

REFERENCES

[1] Y. Sun, C. Zhang, Y. Yang, H. Ma, and Y. Sun, "Improving the color gamut of a liquid-crystal display by using a bandpass filter," *Curr. Opt. Photonics*, vol. 3, no. 6, pp. 590–596, 2019, doi: 10.3807/COPP.2019.3.6.590.

[2] L. Zhao, J. Mao, B. Jiang, X. Wei, Y. Chen, and M. Yin, "Temperature-dependent persistent luminescence of $SrAl_2O_4$:Eu^{2+}, Dy^{3+}, Tb^{3+}: a strategy of optical thermometry avoiding real-time excitation," *Opt. Lett.*, vol. 43, no. 16, p. 3882, Aug. 2018, doi: 10.1364/OL.43.003882.

[3] Y. Wang, Y. Liu, J. Shen, X. Wang, and X. Yan, "Controlling optical temperature behaviors of Er^{3+} doped Sr_2CaWO_6 through doping and changing excitation powers," *Opt. Mater. Express*, vol. 8, no. 7, p. 1926, Jul. 2018, doi: 10.1364/OME.8.001926.

[4] Z. Li, Y. Tang, J. Li, X. Ding, C. Yan, and B. Yu, "Effect of flip-chip height on the optical performance of conformal white-light-emitting diodes," *Opt. Lett.*, vol. 43, no. 5, p. 1015, Mar. 2018, doi: 10.1364/OL.43.001015.

[5] D. Yan, S. Zhao, H. Wang, and Z. Zang, "Ultrapure and highly efficient green light emitting devices based on ligand-modified CsPbBr 3 quantum dots," *Photonics Res.*, vol. 8, no. 7, p. 1086, Jul. 2020, doi: 10.1364/PRJ.391703.

[6] J. Cao, J. Zhang, and X. Li, "Upconversion luminescence of $Ba_3La(PO_4)_3$:Yb^{3+}-Er^{3+} /Tm^{3+} phosphors for optimal temperature sensing," *Appl. Opt.*, vol. 57, no. 6, p. 1345, Feb. 2018, doi: 10.1364/AO.57.001345.

[7] M. Gupta, A. K. Dubey, V. Kumar, and D. S. Mehta, "Indoor daylighting using Fresnel lens solar-concentrator-based hybrid cylindrical luminaire for illumination and water heating," *Appl. Opt.*, vol. 59, no. 18, p. 5358, Jun. 2020, doi: 10.1364/AO.389044.

[8] Y.-D. Chen, J.-C. Wang, J.-H. Zhang, and G.-Y. Cao, "Light source for comfortable lighting and trapping pests in tea gardens based on solar-like lighting," *Appl. Opt.*, vol. 59, no. 27, p. 8459, Sep. 2020, doi: 10.1364/AO.398075.

[9] L. Xiao, C. Zhang, P. Zhong, and G. He, "Spectral optimization of phosphor-coated white LED for road lighting based on the mesopic limited luminous efficacy and IES color fidelity index," *Appl. Opt.*, vol. 57, no. 4, p. 931, Feb. 2018, doi: 10.1364/AO.57.000931.

[10] S. Bindai, K. Annapurna, and A. Tarafder, "Realization of phosphor-in-glass thin film on soda-lime silicate glass with low sintering temperature for high color rendering white LEDs," *Appl. Opt.*, vol. 58, no. 9, p. 2372, Mar. 2019, doi: 10.1364/AO.58.002372.
[11] K. Huraibat, E. Perales, E. Kirchner, I. V. der Lans, A. Ferrero, and J. Campos, "Accurate physics-based digital reproduction of effect coatings," *Opt. Express*, vol. 29, no. 21, p. 34671, Oct. 2021, doi: 10.1364/OE.438477.
[12] H. S. El-Ghoroury, Y. Nakajima, M. Yeh, E. Liang, C.-L. Chuang, and J. C. Chen, "Color temperature tunable white light based on monolithic color-tunable light emitting diodes," *Opt. Express*, vol. 28, no. 2, p. 1206, Jan. 2020, doi: 10.1364/OE.375320.
[13] A. Kho and V. J. Srinivasan, "Compensating spatially dependent dispersion in visible light OCT," *Opt. Lett.*, vol. 44, no. 4, p. 775, Feb. 2019, doi: 10.1364/OL.44.000775.
[14] L. Frey *et al.*, "High-performance silver-dielectric interference filters for RGBIR imaging," *Opt. Lett.*, vol. 43, no. 6, p. 1355, Mar. 2018, doi: 10.1364/OL.43.001355.
[15] S. Elmalem, R. Giryes, and E. Marom, "Learned phase coded aperture for the benefit of depth of field extension," *Opt. Express*, vol. 26, no. 12, p. 15316, Jun. 2018, doi: 10.1364/OE.26.015316.
[16] B. Zhang *et al.*, "Rapid, large-scale stimulated Raman histology with strip mosaicing and dual-phase detection," *Biomed. Opt. Express*, vol. 9, no. 6, p. 2604, Jun. 2018, doi: 10.1364/BOE.9.002604.
[17] H. Kim, Y.-J. Seo, and Y. Kwak, "Transparent effect on the gray scale perception of a transparent OLED display," *Opt. Express*, vol. 26, no. 4, p. 4075, Feb. 2018, doi: 10.1364/OE.26.004075.
[18] M. M. Magno-Canto, L. I. W. McKinna, B. J. Robson, and K. E. Fabricius, "Model for deriving benthic irradiance in the Great Barrier Reef from MODIS satellite imagery," *Opt. Express*, vol. 27, no. 20, p. A1350, Sep. 2019, doi: 10.1364/OE.27.0A1350.
[19] D. Durmus and W. Davis, "Blur perception and visual clarity in light projection systems," *Opt. Express*, vol. 27, no. 4, p. A216, Feb. 2019, doi: 10.1364/OE.27.00A216.
[20] Q. Zaman *et al.*, "Two-color surface plasmon resonance nanosizer for gold nanoparticles," *Opt. Express*, vol. 27, no. 3, p. 3200, Feb. 2019, doi: 10.1364/OE.27.003200.
[21] Y. Li, X. Zhang, H. Yang, X. Yi, J. Wang, and J. Li, "Effects of remote sediment phosphor plates on high power laser-based white light sources," *Opt. Express*, vol. 29, no. 15, p. 24552, Jul. 2021, doi: 10.1364/OE.433581.
[22] Y.-P. Chang *et al.*, "New scheme of LiDAR-embedded smart laser headlight for autonomous vehicles," *Opt. Express*, vol. 27, no. 20, p. A1481, Sep. 2019, doi: 10.1364/OE.27.0A1481.
[23] A. A. Pan'kov, "Informative light pulses of indicating polymer fiber-optic piezoelectroluminescent coatings upon indentation of rigid globular particles," *J. Opt. Technol.*, vol. 88, no. 8, p. 477, Aug. 2021, doi: 10.1364/JOT.88.000477.
[24] I. Fujieda, Y. Tsutsumi, and S. Matsuda, "Spectral study on utilizing ambient light with luminescent materials for display applications," *Opt. Express*, vol. 29, no. 5, p. 6691, Mar. 2021, doi: 10.1364/OE.418869.
[25] J. Zhou and K. Qian, "Low-voltage wide-field-of-view lidar scanning system based on a MEMS mirror," *Appl. Opt.*, vol. 58, no. 5, p. A283, Feb. 2019, doi: 10.1364/AO.58.00A283.

BIOGRAPHIES OF AUTHORS

Ha Thanh Tung received the Ph.D. degree in physics from University of Science, Vietnam National University Ho Chi Minh City, Vietnam, he is working as a lecturer at the Faculty of Basic Sciences, Vinh Long University of Technology Education, Vietnam. His research interests focus on developing the patterned substrate with micro- and nano-scale to apply for physical and chemical devices such as solar cells, OLED, photoanod. He can be contacted at email: tunght@vlute.edu.vn.

Huu Phuc Dang received a Physics Ph.D. degree from the University of Science, Ho Chi Minh City, in 2018. Currently, he is a lecturer at the Faculty of Fundamental Science, Industrial University of Ho Chi Minh City, Ho Chi Minh City, Vietnam. His research interests include simulation LEDs material, renewable energy. He can be contacted at email: danghuuphuc@iuh.edu.vn.